Available online at www.sciencedirect.com
SCIENCE DIRECT®
Journal of Magnetic Resonance 167 (2004) 36–41
JMR Journal of Magnetic Resonance
www.elsevier.com/locate/jmr

Analysis of multi-exponential relaxation data with very short components using linear regularization☆

Jonathan B. Moody and Yang Xia*

Department of Physics, Oakland University, 190 Science and Engineering Building, Rochester, MI 48309-4487, USA

Received 4 September 2003; revised 17 November 2003

Abstract

Linear regularization is a common and robust technique for fitting multi-exponential relaxation decay data to obtain a distribution of relaxation times. The regularization algorithms employed by the Uniform-Penalty inversion (UPEN) and CONTIN computer programs have been compared using simulated transverse (T_2) relaxation data derived from a typical bimodal distribution observed in cartilage tissue which contain a component shorter than t_0, the time of the first decay sample. We examined the reliability of detecting sub-t_0 relaxation components and the accuracy of statistical estimates of T_2 distribution parameters. When the integrated area of the sub-t_0 component relative to that of the total distribution was greater than 0.25, our results indicated a signal-to-noise threshold of about 300 for detecting the presence of the sub-t_0 component with a probability of 0.9 or greater. This threshold was obtained using both the UPEN and CONTIN algorithms. In addition, when using the second-derivative-squared regularizer, UPEN solutions provided statistical estimates of T_2 distribution parameters which were substantially free of the biasing effect of the regularizer observed in analagous CONTIN solutions.

Keywords: Linear regularization; Multi-exponential decay; T_2 relaxation; Simulated T_2 data; Cartilage

1. Introduction

Multi-exponential transverse (T_2) relaxation is often encountered in relaxation studies of biological tissues and other heterogeneous systems. One popular and robust method of analysis makes use of various computer implementations of linear regularization techniques to fit the decay data and obtain a continuous distribution of relaxation components characteristic of the tissue [1–6].

In multi-exponential T_2 studies of diverse biological tissues such as muscle, cartilage, tendon, and brain, many investigators have reported a liquid-like relaxation component with mean T_2 in the range 0.4–5 ms and there is evidence that this component may be partially associated with protons of relatively mobile macromolecules [2,7–10,19,20]. This short component is generally observable under bulk spectroscopic conditions (i.e., without spatial localization), but under conditions of imaging or spatially resolved spectroscopy, may be partially or wholly decayed away due to longer echo times.

When fitting T_2 relaxation data, it has been common practice to exclude relaxation components that occur below t_0, the time of the first acquired spin echo [4]. However, if the signal-to-noise ratio (SNR) is high enough and the time interval between the mean of the fast T_2 component and t_0 is not too great, a certain amount of extrapolation below t_0 is generally allowable because a portion of the sub-t_0 relaxation component may still be present in the earliest data points before dropping below the noise level. Here we examine the accuracy of such an extrapolation as well as the detectability of sub-t_0 components using simulations of smooth two-component relaxation distributions under varying conditions of SNR and component fractional weight (i.e., integrated component area relative to that of the total distribution). The simulated data were fitted using two different regularization algorithms to find optimized

☆ *Source of support*. Research Excellence Fund in Biotechnology from Oakland University (Y.X.). An instrument endorsement from R.B. and J.N. Bennett (Y.X.). R01 Grant (AR 45172) from NIH (Y.X.)
* Corresponding author. Fax: 1-248-370-3408.
E-mail address: xia@oakland.edu (Y. Xia).

1090-7807/$ - see front matter © 2003 Elsevier Inc. All rights reserved.
doi:10.1016/j.jmr.2003.11.004

regularization conditions. An approximate threshold for the detection of sub-t_0 components was determined and we found that a statistical sampling of T_2 decays with similar underlying relaxation distributions provides reasonable estimates of sub-t_0 component fractional weight and mean T_2. This approach has found application in spatially localized multi-exponential T_2 mapping of cartilage using T_2-weighted microscopic MR line-scans (J.B. Moody, unpublished data).

2. Methods

Simulated decay data were generated using conditions similar to actual T_2-weighted line-scan experiments in cartilage. The simulated T_2 distributions, $g(T_2)$, consisted of two components with mean values of 0.55 and 29 ms. Each component was simulated as a gaussian distribution of half-width (second moment) approximately 5% of the component mean [6,13]. The relatively narrow simulated component widths were chosen on the basis of T_2 distributions from actual experimental data in cartilage (these narrow components in cartilage may be a consequence of the high spatial resolution and small tissue volume ($0.014\,\mathrm{mm}^3$) represented in each voxel of the line-scan) (J.B. Moody, unpublished data). The initial transverse magnetization M_0 (zeroth moment of the distribution) was calculated as

$$M_0 = \int_{T_2^{\mathrm{i}}}^{T_2^{\mathrm{f}}} g(T_2)\,\mathrm{d}T_2, \tag{1}$$

where the integration limits $[T_2^{\mathrm{i}}, T_2^{\mathrm{f}}]$ cover the range of T_2 where nonzero distribution components are expected; in all simulations, the integration limits were fixed at [0.1 ms, 1 s]. The fractional weights (zeroth moment), P_j, of the T_2 components were defined by

$$P_j = (1/M_0) \int_{T_{2j}^{\mathrm{i}}}^{T_{2j}^{\mathrm{f}}} g(T_2)\,\mathrm{d}T_2, \quad j = a, b, \tag{2}$$

where a and b signify the shorter and longer components, respectively, and the integration limits $[T_{2j}^{\mathrm{i}}, T_{2j}^{\mathrm{f}}]$, extend over the T_2 interval covered by the jth component. For each simulated distribution, M_0 was normalized to unity, and P_a was varied between 0.25 and 0.75 ($P_b = 1 - P_a$).

The simulated decay data were sampled at 80 time points by numerically integrating,

$$s(t_k) = \int_{T_2^{\mathrm{i}}}^{T_2^{\mathrm{f}}} g(T_2) \exp(-t_k/T_2)\,\mathrm{d}T_2, \quad k = 1, \ldots, 80. \tag{3}$$

In the time domain a quasi-logarithmic sampling scheme was used: the first approximately 40 points were sampled at intervals of 4τ (these are the first 40 even echoes where $\tau = 0.4$ ms is the 90°–180° interpulse delay of a Carr–Purcell–Meiboom–Gill (CPMG) pulse sequence [21]. The remainder of the data points were sampled in approximately equally spaced intervals of $\log(t_k)$ such that t_k was an even multiple of τ. The transition between the two sampling rates occurred at approximately 80 ms by which time the signal had decayed to about 1–4% of its initial value. The total time interval covered by the decay data was from 1.6 to 6 s (the log-spaced portion of the sampling scheme was generated using the full time interval, and all time points before 80 ms were discarded). Zero mean pseudo-random noise with a gaussian distribution was added to the simulated decay data. The variance of the noise was adjusted so that the SNR of the simulated data varied between 100 and 600, where SNR is the initial signal amplitude divided by the standard deviation of the last 15% of the data points in the decay tail. Thus, the sampling scheme allowed efficient sampling of the baseline standard deviation at long times, while providing a sufficiently high sampling rate at short times, within the constraint of an 80-point total decay sample.

2.1. Analysis of solutions

For each combination of SNR and P_a, a group 100 simulated data sets was generated and fitted using our own implementation of the Uniform-Penalty (UPEN) regularization algorithm [1] written in the Python (www.python.org), a freely available general purpose programming language with numeric capabilities similar to Matlab or IDL. Identically generated simulated data were also fitted using the Fortran program CONTIN [11,12]. In each case, we tested two forms of the regularizer, the second derivative-squared and the amplitude-squared of the solution; a non-negativity constraint was applied in all cases [1,11]. In the calculated solutions, all components with fractional weight greater than 1% were included in the analysis. The solutions were evaluated in two ways: first, the probability of obtaining a solution with the correct number of components (the "admissibility" [13]) was calculated; and second, for each distribution component, the fractional weight (Eq. (2)) and mean T_2

$$\langle T_{2j} \rangle = \int_{T_{2j}^{\mathrm{i}}}^{T_{2j}^{\mathrm{f}}} g(T_2) T_2\,\mathrm{d}T_2, \quad j = a, b, \tag{4}$$

were determined, as well as the mean and standard deviation of these parameters over each group of 100 similar data sets. Normality of the group data was checked with the Shapiro–Wilk normality test [14] and the group means were compared with the true distribution parameters.

3. Results

In Figs. 1A and B, the admissibility (probability of obtaining the correct number of relaxation components)

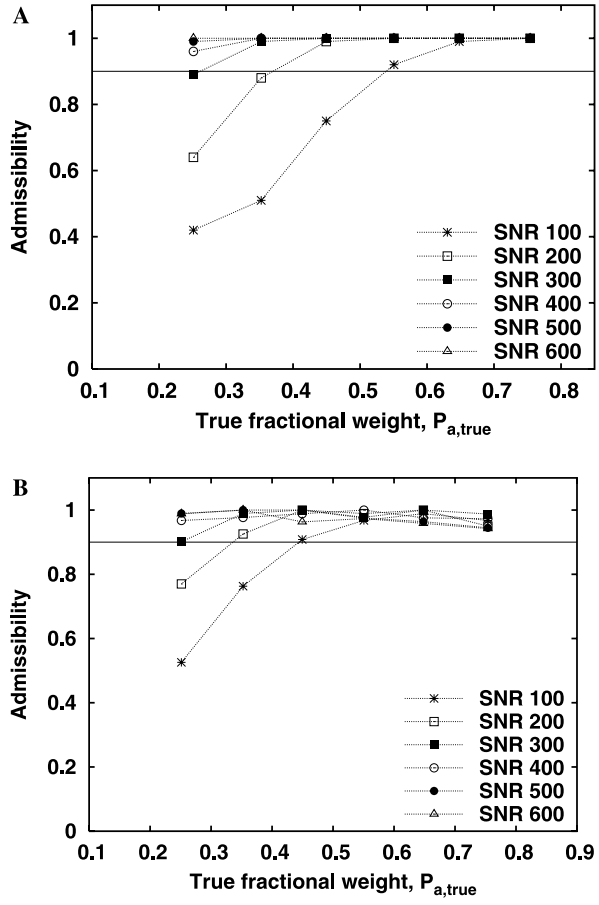

Fig. 1. The admissibility (probability of obtaining the correct number of relaxation components) as a function of $P_{a,\text{true}}$, the true fractional weight of the short T_2 component, for six values of the signal-to-noise ratio (SNR). Each point was determined from solutions of 100 simulated T_2 data sets which were identical apart from added gaussian pseudo-random noise. Solutions were calculated using CONTIN (A) and UPEN (B) programs. The horizontal line indicates a probability of 0.9.

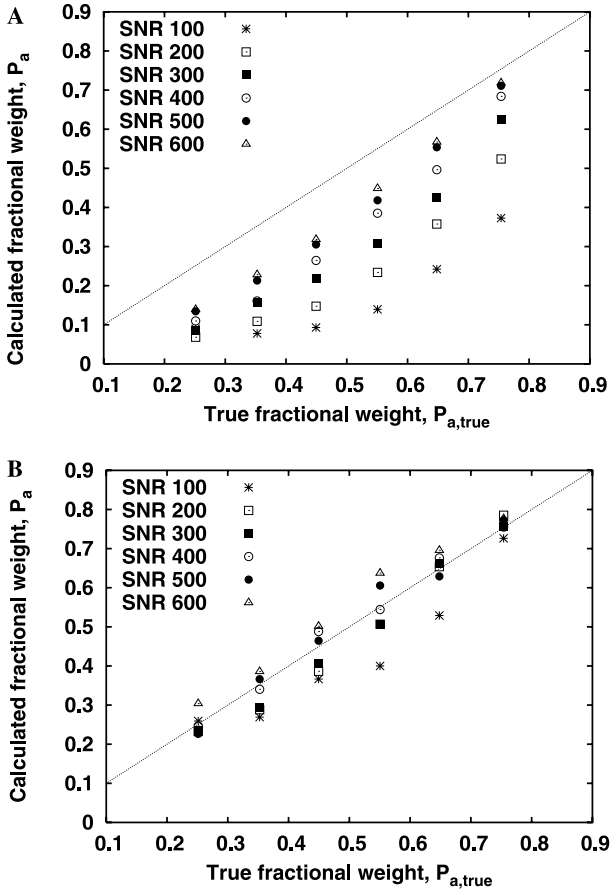

Fig. 2. The calculated fractional weight, P_a, of the short T_2 component as a function of $P_{a,\text{true}}$, the true fractional weight of the short T_2 component, for six values of the signal-to-noise ratio (SNR). Solutions were calculated using CONTIN (A) and UPEN (B) programs. The plotted line represents $P_a = P_{a,\text{true}}$. For CONTIN solutions (A) the standard deviations ranged from 0.35 to 0.73 for $P_{a,\text{true}}$ of 0.75 and from 0.04 to 0.09 for $P_{a,\text{true}}$ of 0.25. For UPEN solutions (B) the standard deviations ranged from 0.13 to 0.22 for $P_{a,\text{true}}$ of 0.75 and from 0.19 to 0.23 for $P_{a,\text{true}}$ of 0.25.

as a function $P_{a,\text{true}}$ is shown for CONTIN and UPEN solutions, respectively. Similar results were seen in the two cases: when SNR was greater than 300 and P_a greater than 0.25, the admissibility was greater than 90%. The calculated P_a versus $P_{a,\text{true}}$ is shown in Figs. 2A and B for CONTIN and UPEN solutions, respectively. The points are means for each group of 100 simulated data sets with given SNR and $P_{a,\text{true}}$ and the line represents $P_a = P_{a,\text{true}}$. The values of P_b from UPEN solutions are somewhat scattered symmetrically about the line (Fig. 2B), but values from CONTIN solutions are all significantly underestimated (Fig. 2A). Similarly, the calculated mean values of T_{2a} were consistently overestimated for CONTIN solutions (Fig. 3A) (the horizontal line represents the true T_{2a}), but were generally closer to the true T_{2a} for UPEN solutions (Fig. 3B). The standard deviations of T_{2a} and P_a for each group of 100 simulated datasets with fixed SNR and $P_{a,\text{true}}$ were about 10% for CONTIN solutions compared to about 30–40% for UPEN solutions. The values of T_{2b} for both CONTIN and UPEN solutions were within about 0.2 ms of the true value (data not shown). P_b showed characteristics very similar to P_a, since it is linearly dependent on P_a (data not shown). The results shown in Figs. 1–3 were from solutions using the second derivative-squared regularizer; the amplitude-squared regularizer for both UPEN and CONTIN algorithms was unable to produce accurate statistical estimates of distribution parameters (not shown). The results of the Shapiro–Wilk normality test indicated that the statistical distribution of all relaxation parameters (T_{2a}, T_{2b}, P_a, and P_b) deviated significantly from normality ($p < 0.001$).

4. Discussion

Using a model relaxation distribution with gaussian components at 0.55 and 29 ms, we simulated T_2 decay

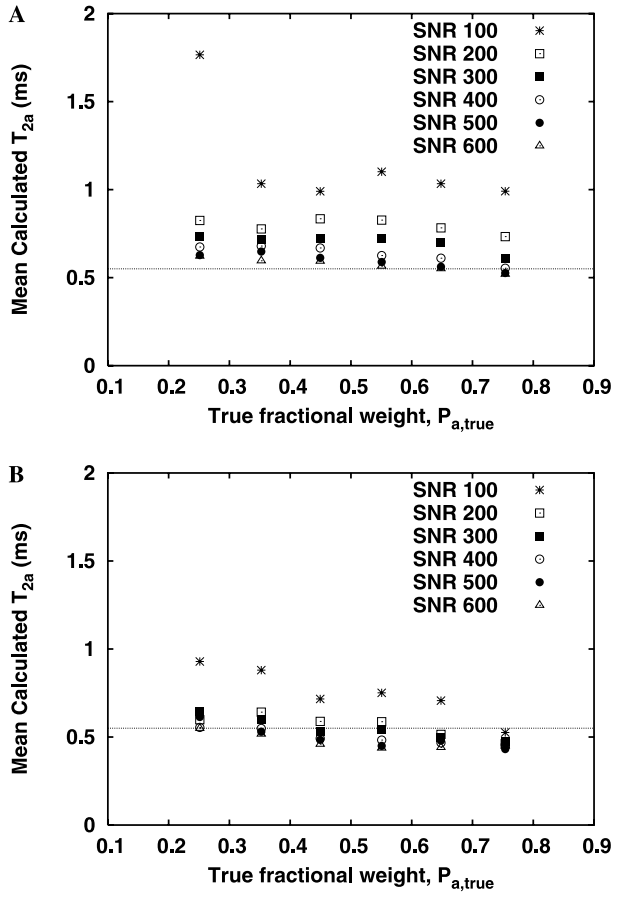

Fig. 3. The mean calculated T_{2a} of the short T_2 component as a function of $P_{a,\text{true}}$, the true fractional weight of the short T_2 component, for six values of the signal-to-noise ratio (SNR). Solutions were calculated using (A) CONTIN and (B) UPEN programs. The plotted line represents the true value, $T_{2b} = 0.55$ ms. For CONTIN solutions (A) the standard deviations ranged from 0.52 to 0.97 ms for $P_{a,\text{true}}$ of 0.75 and from 0.48 to 0.88 ms for $P_{a,\text{true}}$ of 0.25. For UPEN solutions (B) the standard deviations ranged from 0.08 to 0.27 ms for $P_{a,\text{true}}$ of 0.75 and from 0.26 to 1.2 ms for $P_{a,\text{true}}$ of 0.25.

data with a range of component fractional weights and SNR. The mean T_2 of the short component was selected to be less than t_0 ($= 1.6$ ms), the time of the first simulated decay data point in order to investigate the validity and accuracy of extrapolating the solution below t_0. In general, the T_2 decay must be sampled at a rate, $\tau_s^{-1} = T_{2a}^{-1}$, where T_{2a} is the shortest T_2 component that may occur in the distribution, and the decay must be sampled over a time interval covering the full range of possible relaxation components. For a typical experiment, this implies at least 1000 decay samples over a time interval from 1 ms to 1–5 s, and an echo time, TE, between 1 and 5 ms. These sampling requirements may be relaxed somewhat if at later times we do not acquire all echoes in the CPMG echo-train, but only those that are spaced logarithmically in time. This may reduce significantly the total number of data points necessary to sample the entire decay as well as the total acquisition time.

Signal-to-noise requirements vary depending on the characteristics of the underlying T_2 distribution; resolving two components with T_2 values within a factor of 2–3 of each other may require a SNR more than an order of magnitude higher than resolving more widely separated components; and conversely, resolving components with widely different fractional weights also requires much higher SNR than equally weighted components [6]. In our simulations the two model components were separated by more than a factor of 50, so that SNR was more important in determining the accuracy of the shorter component.

One way these stringent sampling and SNR requirements have been achieved in vivo is by using localized spectroscopy methods to measure multi-exponential T_2 distributions in large voxels, trading spatial resolution for temporal resolution, with echo-times on the order of 1 ms [2,3]. Another approach, 1-dimensional (1-D) line-scan imaging, retains spatial information along one dimension, with temporal resolution intermediate between that of spatially localized spectroscopic and 2-dimensional (2-D) imaging methods. We have used 1-D line-scan imaging to map multi-exponential T_2 in cartilage and the results will be presented in a forthcoming article .

The UPEN algorithm, like other regularization approaches [11,13,15,16], minimizes a weighted sum of two terms: a linear least-squares term, and a term (the regularizer) involving either the curvature (second derivative squared) or the intensity (amplitude squared) of the solution [1]. Minimization of the first term enforces agreement of the solution with the data while minimization of the regularizer stabilizes the solution against variability due to noise in the data [11]. These two competing effects are balanced by a penalty coefficient, also called the regularization parameter, which selects the relative weight of each term in the weighted sum [17]. The UPEN algorithm is unique compared to other regularization approaches (such as CONTIN) in that it uses a penalty coefficient which is a function of T_2 rather than a constant. This provides a trade-off between the extremes of fitting the data and smoothing which varies continuously as a function of T_2, and allows relaxation distributions with both narrow components and broad tails to be accurately estimated [1].

In our simulations, the probability of obtaining solutions with the correct number of components ("admissibility") was surprisingly high (>90%) when SNR was 300 or better, and this was true of both regularization algorithms tested (Figs. 1A and B). However, the estimates of mean P_a and T_{2a} were significantly better for UPEN solutions (Figs. 2B and 3B) compared to CONTIN solutions (Figs. 2A and 3A). These estimates are means of the distribution parameters for a statistical sample of relaxation decays. Although the estimate of T_{2a} and P_a for any single simulated decay curve

was likely to be inaccurate, the statistical averages for UPEN solutions provided reasonable estimates of the true distribution parameters. This may be applied in multi-exponential T_2 mapping approaches such as MR line-scans, in which some spatial resolution is maintained, or in the case of spatially localized voxel measurements, in which a statistical sample of distinct voxels is available [2]. For experimental data, it is crucial that the first 1–2 data points be free of instrumental artifacts since the estimate of T_{2a} and P_a depends entirely on these points.

Saab et al. [2] have reported reliable detection of a relaxation component with $T_2 < 5$ ms in volume localized CPMG measurements in human skeletal muscle, although the uncertainties in the short component were somewhat larger than the other four observed components. In that study, the regularization algorithm used was very similar to CONTIN, except that an amplitude-squared form of the regularizer was used; τ was 0.6 ms, SNR was ~3500, and the observed fractional weight of the short component was 11% [2]. In simulations they observed that the fractional weight of the short component was overestimated, while the mean T_2 was underestimated [2].

The significant non-normality of all relaxation parameters (T_{2a}, T_{2b}, P_a, and P_b) indicates the biasing effect of the regularizer as well as the nonlinear relationship between the decay data and the solution due to the non-negativity constraints. Because the data errors are not linearly propagated, conventional estimates of the errors in fitted parameters based on the covariance matrix are not generally valid [11]. Although statistically significant, the bias was not large for the longer T_{2b} component, for which the uncertainty was less than 1% for both UPEN and CONTIN solutions. However, the much larger effects of the bias on T_{2a} and P_a are evident in the CONTIN solutions (Figs. 2A and 3A). The goal of any regularization algorithm is to apply a strong enough regularizer to find a stable solution, without significantly biasing that solution. The form of the T_2-dependent regularizer in the UPEN algorithm is reminiscent of the locally adaptive iterative inversion discussed by Biemond et al. [18] in the application of 2-D regularization to image deblurring. Because the UPEN penalty coefficient adapts to the local characteristics of the solution, the algorithm is able to simultaneously accommodate both narrow components and broad tails, as well as weakly (sub-t_0) and strongly (e.g., T_{2b}) represented components.

Although the UPEN algorithm using the second derivative-squared regularizer seems to provide better statistical estimates of very fast relaxation components, we have observed both in simulations and in cartilage relaxation data that the amplitude-squared regularizer seems to do better at resolving closely spaced relaxation components separated by a factor of 2–3. This emphasizes the fact that one set of regularization conditions is unlikely to perform well in all cases, and that multiple algorithms are necessary in order to find the best interpretation of a given relaxation data set [16].

In summary, for simulated bimodal relaxation data which contain a component shorter than t_0 (the time of the first decay sample), when SNR was greater than 300 and P_a was greater than 0.25, the probability of obtaining the correct number of relaxation components was 0.9 or greater. This was obtained using both the UPEN and CONTIN regularization algorithms. In addition, when using the second derivative-squared regularizer, UPEN solutions provided statistical estimates of relaxation distribution parameters which were substantially free of the biasing effect of the regularizer which was observed in analogous solutions found by the CONTIN program.

Acknowledgments

We thank Dr. R.J.S. Brown for providing the source code of the original UPEN implementation, and for helpful discussions.

References

[1] G. Borgia, R. Brown, P. Fantazzini, Uniform-penalty inversion of multiexponential decay data. II. Data spacing, T_2 data, systematic data errors, and diagnostics, J. Magn. Reson. 147 (2000) 273–285.
[2] G. Saab, R. Thompson, G.D. Marsh, Multicomponent T_2 relaxation of in vivo skeletal muscle, Magn. Reson. Med. 42 (1999) 150–157.
[3] S.J. Graham, M.J. Bronskill, MR measurement of relative water content and multicomponent T_2 relaxation in human breast, Magn. Reson. Med. 35 (1996) 706–715.
[4] R.M. Henkelman, G.J. Stanisz, J.K. Kim, M.J. Bronskill, Anisotropy of NMR properties of tissues, Magn. Reson. Med. 32 (1994) 592–601.
[5] K.P. Whittall, M.J. Bronskill, R.M. Henkelman, Investigation of analysis techniques for complicated NMR relaxation data, J. Magn. Reson. 95 (1991) 221–234.
[6] R.M. Kroeker, R.M. Henkelman, Analysis of biological NMR data with continuous distribution of relaxation times, J. Magn. Reson. 69 (1986) 218–235.
[7] C.F. Hazlewood, D.C. Chang, B.L. Nichols, D.E. Woessner, Nuclear magnetic resonance transverse relaxation times of water protons in skeletal muscle, Biophys. J. 14 (1974) 583–606.
[8] B. Fung, P.S. Puon, Nuclear magnetic resonance transverse relaxation in muscle water, Biophys. J. 33 (1981) 27–38.
[9] T. Mosher, B. Dardzinski, M. Smith, Characterization of multiple T_2 components in articular cartilage, in: 5th Scientific Meeting, ISMRM, Vancouver, 1997.
[10] P.J. Lattanzio, K.W. Marshall, A.Z. Damyanovich, H. Peemoeller, Macromolecule and water magnetization exchange modeling in articular cartilage, Magn. Reson. Med. 44 (2000) 840–851.
[11] S.W. Provencher, A constrained regularization method for inverting data represented by linear algebraic or integral equations, Comp. Phys. Commun. 27 (1982) 213–227.

[12] S.W. Provencher, CONTIN: a general purpose constrained regularization program for inverting noisy linear algebraic and integral equations, Comp. Phys. Commun. 27 (1982) 229–242.
[13] S.J. Graham, P.L. Stanchev, M.J. Bronskill, Criteria for analysis of multicomponent tissue T_2 relaxation data, Magn. Reson. Med. 35 (1996) 370–378.
[14] J.P. Royston, An extension of Shapiro and Wilk's W test for normality to large samples, Appl. Stat. 31 (1982) 115–124.
[15] J. Weese, A reliable and fast method for the solution of Fredholm integral equations of the first kind based on Tikhonov regularization, Comp. Phys. Commun. 69 (1992) 99–111.
[16] K.P. Whittall, A.L. MacKay, Quantitative interpretation of NMR relaxation data, J. Magn. Reson. 84 (1989) 134–152.
[17] W.H. Press, S.A. Teukolsky, W.T. Vetterling, B.P. Flannery, Numerical Recipes in Fortran 77: The Art of Scientific Computing, Cambridge University Press, Cambridge, 1992.
[18] J. Biemond, R.L. Lagendijk, R.M. Mersereau, Iterative methods for image deblurring, Proc. IEEE 78 (1990) 856–883.
[19] H.W. Fischer, P.A. Rinck, Y. Van Haverbeke, R.N. Muller, Nuclear relaxation of human brain gray and white matter: analysis of field dependence and implications for MRI, Magn. Reson. Med. 16 (1990) 317–334.
[20] S. Peto, P. Gillis, V.P. Henri, Structure and dynamics of water in tendon from NMR relaxation measurements, Biophys. J. 57 (1990) 71–84.
[21] S. Meiboom, D. Gill, Modified spin-echo method for measuring nuclear relaxation, Rev. Sci. Instrum. 29 (1958) 668–691.